

SPECIAL ISSUE PAPER

The role of stomatal acclimation in modelling tree adaptation to high CO₂

Thomas N. Buckley^{1,2,3,*}¹ School of Biological, Earth and Environmental Sciences, University of New South Wales, Sydney NSW 2052, Australia² Bushfire Cooperative Research Centre, Australia³ Ensis, PO Box E4008, Kingston ACT 2604, Australia

Received 21 June 2007; Revised 2 September 2007; Accepted 4 September 2007

Abstract

Carbon dioxide enrichment changes the balance of photosynthetic limitations due to water, nitrogen, and light. This paper examines the role of stomata in these changes by comparing enrichment responses predicted by an optimality-based tree growth model, DESPOT, using three alternative 'setpoints' for stomatal acclimation: leaf water potential (ψ_l -setpoint), the ratio of intercellular to ambient CO₂ mole fraction (c_i/c_a -setpoint), and the parameters in a simple model in which stomata are controlled by H₂O and CO₂ supply and demand (linked feedback). In each scenario, stomatal conductance (g_s) and photosynthetic capacity (V_m) declined, productivity and leaf area index (LAI) increased, and c_i/c_a remained within 5% of its pre-enrichment value. Height growth preceded the LAI response in the ψ_l -setpoint and linked feedback scenarios, but not in the c_i/c_a -setpoint scenario. These trends were explained in terms of photosynthetic resource substitution using the equimarginal principle of production theory, which controls carbon allocation in DESPOT: enrichment initially increased the marginal product for light, driving substitution towards light; height growth also drove substitution towards N in the ψ_l and feedback scenarios, but the inflexibility of c_i/c_a prevented that substitution in the c_i/c_a scenario, explaining the lack of height response. Each scenario, however, predicted similar behaviour for c_i/c_a and carbon and water flux. These results suggest that 'setpoints' may be robust tools for linking and constraining carbon and water fluxes, but that they should be used more cautiously in predicting or interpreting how those fluxes arise from changes in tree structure and physiology.

Key words: Carbon dioxide, climate change, photosynthesis, stomata, transpiration, water potential.

Introduction

A major challenge facing plant biologists today is the need for confident predictions about plant responses to climate change, based on sound theoretical understanding and supported by experiment where possible (Steffen and Canadell, 2005). This need is especially important for trees, because forests dominate the terrestrial biosphere, in terms of both carbon stocks and carbon fluxes. However, it is also especially difficult for trees, because the long lifespans of many species make it impossible to document experimentally the long-term effects of CO₂ enrichment above present-day levels. This makes long-term forecasting of tree growth and gas exchange heavily dependent on assumptions about the character of adaptive growth regulation.

One hallmark of plant growth is the strong co-ordination between structural development and physiological functioning, often described as 'functional balance', for example, between sapwood and leaf area (Shinozaki *et al.*, 1964a, b) or roots and shoots (Davidson, 1969; Thornley, 1972a, b). Many growth models incorporate functional balance as a central constraint to predict carbon allocation and thus structural adjustment (Valentine, 1985, 1999; Mäkelä, 1986, 1997, 1999; Hilbert and Reynolds, 1991; Deleuze and Houllier, 1995; Luan *et al.*, 1996; Grote, 1998; Lo *et al.*, 2001; Battaglia *et al.*, 2004). The dynamic regulation of leaf gas exchange is also characterized by functional balance: stomatal behaviour co-ordinates CO₂ supply with photosynthetic demand and evaporative

* To whom correspondence should be addressed at Ensis, PO Box E4008, Kingston ACT 2604 Australia. E-mail: tom_buckley@alumni.jmu.edu

demand with hydraulic supply, leading to virtually homeostatic control of both c_i/c_a (intercellular/ambient [CO₂]) and leaf water potential, ψ_l (Wong *et al.*, 1979, 1985a, b; Farquhar and Sharkey, 1982; Jones, 1990; Tardieu, 1993; Saliendra *et al.*, 1995) (a list of symbols with definitions and dimensions is given in Table 1). These functional balancing acts—of structural adaptation and stomatal regulation—are deeply entangled with one another. Homeostatic control of c_i/c_a depends as much on the co-ordination of root, stem, and leaf production as it does on stomatal responses to the leaf environment, because those structural features determine the relative supplies of nitrogen, water, and light needed for photosynthesis.

Very little is known, however, about how the ‘setpoints’ for ψ_l and c_i/c_a are controlled, or about their potential to change systematically over long time scales in relation to the environmental and structural effectors of photosynthetic resource balance (Farquhar *et al.*, 1989; Ehleringer and Cerling, 1995; Miller *et al.*, 2001; Miller, 2002). The data that are available paint a varied and often contradictory picture. For example, Barnard and Ryan (2003) found that the hydraulic burdens created by height growth in *Eucalyptus saligna* were compensated by structural adjustment of sapwood:leaf area ratio and down-regulation of the ψ_l -setpoint, which sustained stomatal conductance, g_s , with the result that the c_i/c_a -setpoint was not lower in taller, older trees (it was slightly higher, in fact). In contrast, Phillips *et al.* (2003) found large reductions in g_s ,

ψ_l and c_i/c_a in 25 m tall Oregon white oak (*Quercus garryana* Dougl. ex. Hook) as compared with 10 m tall trees. Wide ranges of compensation have been reported for each of these parameters in relation to height growth for various species (Ryan *et al.*, 2006).

Carbon dioxide enrichment is similar to height growth in that it drives a complicated series of interacting changes in tree structure and function (Norby *et al.*, 1999; Korner *et al.*, 2005; Hyvonen *et al.*, 2007) that are particularly difficult to disentangle because of the long time scales over which they occur. Most of what we know about how trees will adapt to high CO₂ is based on observed responses to a few years of CO₂ enrichment (Ainsworth and Long, 2005; Norby *et al.*, 2005). Although trees suddenly exposed to elevated CO₂ typically gain more carbon to begin with, they may not distribute the extra carbon among roots, leaves, and other carbon pools in the same proportions as they did before enrichment (Norby *et al.*, 1999; Korner, 2006; Hyvonen *et al.*, 2007). The actual patterns of carbon reinvestment, combined with any changes in the apparent setpoints for stomatal control, will ultimately determine how tree carbon–water balance responds to CO₂ enrichment over many decades and centuries.

The purpose of this paper is to examine the effect of alternative hypotheses about the long-term ‘setpoints’ for stomatal acclimation on predictions of adaptive tree responses to CO₂ enrichment. Tree growth was simulated at elevated CO₂ using a model, DESPOT (Buckley and Roberts, 2006a), in which carbon allocation is governed by the equimarginal principle of production theory, and carbon gain is calculated from a big-leaf Farquhar *et al.* (1980) model with stomatal conductance prescribed by one of three alternative ‘setpoint’ hypotheses. These simulations were assessed in relation to enrichment responses reported for trees in FACE (free-air CO₂ enrichment) experiments, and the patterns predicted for structural and physiological adaptation under each acclimation scenario were analysed in terms of photosynthetic resource substitution using the equimarginal principle.

Outline of the approach

The response of mature trees to a step increase in ambient CO₂ mole fraction (c_a) from 370 ppm to 570 ppm was simulated. This was meant to mimic FACE experiments, to allow the early stages of simulated responses to be compared with empirical data. A tree growth model called DESPOT (Buckley and Roberts, 2006a) was used, which was designed to minimize the influence of *a priori* assumptions about the structural or physiological outcomes of adaptive growth regulation. For example, patterns of height growth, diameter–height relationships, sapwood:leaf area ratios, and root:shoot ratios are not prescribed as empirical constraints. Instead, they emerge from a sequence of carbon allocation decisions that are chosen by

Table 1. List of symbols used in this paper, in order of appearance

Symbols that appear only in the Appendix are defined there.

Name	Symbol	Dimensions
Intercellular CO ₂ mole fraction	c_i	ppm
Ambient CO ₂ mole fraction	c_a	ppm
Bulk leaf water potential	ψ_l	MPa
Stomatal conductance to H ₂ O	g_s	mol air m ⁻² s ⁻¹
Leaf net assimilation rate	A	μmol CO ₂ m ⁻² s ⁻¹
Leaf-level transpiration rate	E	mmol H ₂ O m ⁻² s ⁻¹
Leaf photosynthetic nitrogen content	N	mmol N m ⁻²
Leaf-level incident irradiance (PPFD)	I	μE m ⁻² s ⁻¹
Marginal product for water	μ_e	μmol CO ₂ mmol ⁻¹ H ₂ O
Marginal product for nitrogen	μ_n	μmol CO ₂ s ⁻¹ mmol ⁻¹ N
Marginal product for light	μ_l	μmol CO ₂ μE ⁻¹
Electron transport capacity	J_m	μmol e ⁻ m ⁻² s ⁻¹
Carboxylation capacity	V_m	μmol CO ₂ m ⁻² s ⁻¹
Leaf-specific hydraulic conductance	K_L	mmol H ₂ O m ⁻² s ⁻¹ MPa ⁻¹
Leaf–air H ₂ O vapour mole fraction difference	D	mmol H ₂ O mol ⁻¹ air
Residual photosynthetic capacity	A_r	μmol CO ₂ m ⁻² s ⁻¹
Leaf turgor pressure	P	MPa
Sensitivity of g_s to product of P and A_r	F	mol air MPa ⁻¹ μmol ⁻¹ CO ₂
Maximum leaf turgor pressure	P_m	MPa
Leaf area index	LAI	m ² m ⁻²
Net primary productivity	NPP	kg C m ⁻² s ⁻¹

a numerical algorithm to satisfy a single goal function, which is to maximize carbon gain in the next time step.

How DESPOT responds to CO₂ enrichment

A large step increase of atmospheric CO₂ initiates a cascade of adaptive responses in leaf physiology and plant structure. In order for this adaptive cascade to make the best use of the extra CO₂, in the sense of maximizing the response of net carbon gain, it must satisfy a rule known as the *equimarginal principle* (see any microeconomics text). This principle states that the ratio of *marginal product* (the sensitivity of carbon gain to a given limiting resource, such as water) to *marginal cost* (the additional carbon investment needed to procure more of that limiting resource) should be the same for each photosynthetic resource, provided the responses of carbon gain to each resource, and of each resource to C investment, are convex. The marginal products are defined by Equation 1:

$$\mu_c = \left(\frac{\partial A}{\partial E} \right)_{N,I}, \mu_n = \left(\frac{\partial A}{\partial N} \right)_{E,I}, \mu_i = \left(\frac{\partial A}{\partial I} \right)_{E,N} \quad (1)$$

where A is net CO₂ assimilation rate and E , N , and I are transpiration rate, photosynthetic N content, and incident irradiance, respectively. DESPOT uses a big-leaf approach, so the μ are identical for leaf and canopy level variables. Adaptation to CO₂ enrichment in DESPOT is directed by the equimarginal principle. Because this principle is based on co-ordinating marginal products and marginal costs, which the plant can control via changes in leaf physiology and plant structure, respectively, the adaptations of physiology and structure are also directly co-ordinated in this model. The photosynthetic submodel is thus *implicitly parameterized* by carbon allocation in DESPOT: photosynthetic capacity, incident irradiance, and leaf-specific hydraulic conductance are calculated from structural properties, which in turn emerge from the optimization of carbon allocation with respect to carbon gain.

This leaves two degrees of freedom in the calculations of carbon gain, however: the ratio of electron transport capacity to carboxylation capacity (J_m/V_m) and stomatal conductance. To reduce the analysis presented here to a single degree of freedom, J_m/V_m will be treated as a constant—acknowledging that enrichment often alters this ratio (Ainsworth and Long, 2005), but leaving analysis of those effects for further work and focusing instead on stomatal control. Three alternative assumptions for constraining stomatal conductance will be explored in the present study:

- (i) ψ_1 -setpoint: leaf water potential is assumed invariant over growth time scales. Transpiration is calculated from soil–leaf water potential gradient, given the leaf-specific hydraulic conductance (K_L), which is calculated from structural properties such as sapwood area, fine root biomass, and tree height. g_s is calculated

from the transpiration rate assuming fixed evaporative demand (D). The published form of DESPOT used this assumption, on the grounds that ψ_1 is physically bounded in the negative direction by the threshold for runaway xylem embolism. However, the direct stomatal response to CO₂ enrichment reduces water loss, potentially shifting ψ_1 in the positive direction and thus weakening the rationale for using a fixed ψ_1 to constrain stomatal control in the case of CO₂ enrichment responses. Two other alternatives are outlined below.

- (ii) c_i/c_a -setpoint: the ratio c_i/c_a is assumed to be constant. The assimilation rate, A , is calculated from c_i , given c_a and structurally determined values for irradiance [calculated from leaf area index (LAI) using Beer's Law] and photosynthetic capacity (based on canopy N content, which is simulated dynamically based on uptake by fine roots, N requirements for tissues other than leaves, and senescence losses). g_s is then calculated from A , c_i , and c_a .
- (iii) Linked feedback: stomata respond directly to the balance of both CO₂ and H₂O supply and demand through linked feedback responses, as postulated in the models of Jarvis and Davies (1998) and Buckley *et al.* (2003). Simple measures of the balance of CO₂ and H₂O supply and demand are, respectively, the residual photosynthetic capacity, A_r (the amount A would increase if c_i equalled c_a), and leaf turgor pressure, P . Assuming $g_s = FPA_r$, where F is a parameter, and using $P = P_m - E/K_L = P_m - g_s D/K_L$, where P_m is maximum leaf turgor (osmotic pressure plus soil water potential), this implies

$$g_s = \frac{P_m F K_L A_r}{K_L + D F A_r} \quad (2)$$

In this scenario, the parameters P_m and F are assumed to be conserved by long-term stomatal acclimation, so they are analogous to the 'setpoints' in the other scenarios. Note that the parameter F incorporates both stomatal density and the sensitivity of guard cell osmotic pressure to P and A_r .

Simulations were performed in DESPOT using each of these alternatives, with the following values for each setpoint in their respective simulations: for the ψ_1 -setpoint scenario, $\psi_1 = -1.0$ MPa (the value used in the original publication of DESPOT); for the c_i/c_a -setpoint scenario, $c_i/c_a = 0.65$ (the value from the ψ_1 -setpoint scenario at the time of CO₂ enrichment); and for the linked-feedback scenario, $P_m = 1.2$ MPa and $F = 1.0$ mol air MPa⁻¹ μmol⁻¹ CO₂ (these values were chosen to produce pre-enrichment values of ψ_1 and c_i/c_a similar to those in the other two scenarios). ψ_1 , c_i/c_a , P_m , and F were calculated in each scenario, to determine how these quantities vary when one of them is held constant by assumption. The marginal

products (Eqn 1) were also calculated to illustrate how the economic landscape of tree growth differs under each stomatal acclimation scenario.

Results

Figures 1–5 show the effects predicted by DESPOT for a step increase in atmospheric CO₂ mole fraction (c_a) from 370 ppm to 570 ppm. The initial response is dominated by an increase in height growth (Fig. 1a) in the ψ_1 -setpoint and linked-feedback scenarios, but by an increase in LAI (Fig. 1b) in the c_i/c_a -setpoint scenario. LAI declines in the first year after enrichment in the ψ_1 and feedback scenarios, then increases steadily, whereas height growth never responds significantly in the c_i/c_a scenario. All three scenarios predict decreased allocation to fine roots, whether expressed relative to leaf carbon (Fig. 1c) or sapwood C (Fig. 1d).

All three scenarios also predict declines in stomatal conductance (g_s , Fig. 2a) and photosynthetic capacity [carboxylation capacity, V_m , Fig. 2b (electron transport capacity, J_m , is not independent of V_m in this model)]. Incident photosynthetic irradiance per unit leaf area (I , Fig. 2c) declines immediately in the c_i/c_a scenario, but initially rises in the ψ_1 and feedback scenarios as a result of the initial drop in LAI; irradiance eventually drops below pre-enrichment values in the ψ_1 and feedback cases, but by a smaller amount than g_s or V_m . In all cases, net primary productivity (NPP, Fig. 3a) increases strongly at first before declining somewhat and eventually settling at a stimulation of ~18–21%. Stand-level transpiration (Fig. 3b) declines by 25% in all scenarios after 10 years, before diverging somewhat after 20 years and then converging again such that the net decline after 100 years is 21% for the ψ_1 and c_i/c_a scenarios, and 24% for the feedback scenario (Fig. 3b).

Trajectories for ψ_1 , c_i/c_a , P_m , and F are presented in Fig. 4a–d, respectively; in each panel, one trajectory is simply a horizontal line, representing the simulation in which that parameter was treated as a constant. Leaf water potential increases (moves towards zero) by 5% in the linked-feedback scenario (dashed line in Fig. 4a), or by ~25% in the c_i/c_a -setpoint scenario (dotted line in Fig. 4a). c_i/c_a fluctuates somewhat in the ψ_1 -setpoint scenario before increasing by 3% after 50 years (solid line in Fig. 4a); in the linked-feedback scenario, c_i/c_a declines by 5% after 30 years, but then slowly increases to within 3% of its pre-enrichment value after 50 years. To maintain a fixed setpoint for either ψ_1 or c_i/c_a after enrichment, one of the parameters of the linked-feedback model (Eqn 2) would have to decline: the ψ_1 -setpoint scenario requires either a 6% decline in P_m or a 16% decline in F after 50 years (solid lines in Fig. 4b and c, respectively), whereas the c_i/c_a -setpoint scenario requires declines of 22–29% in P_m or of 50–60% in F (dotted lines in Fig. 4b and c, respectively).

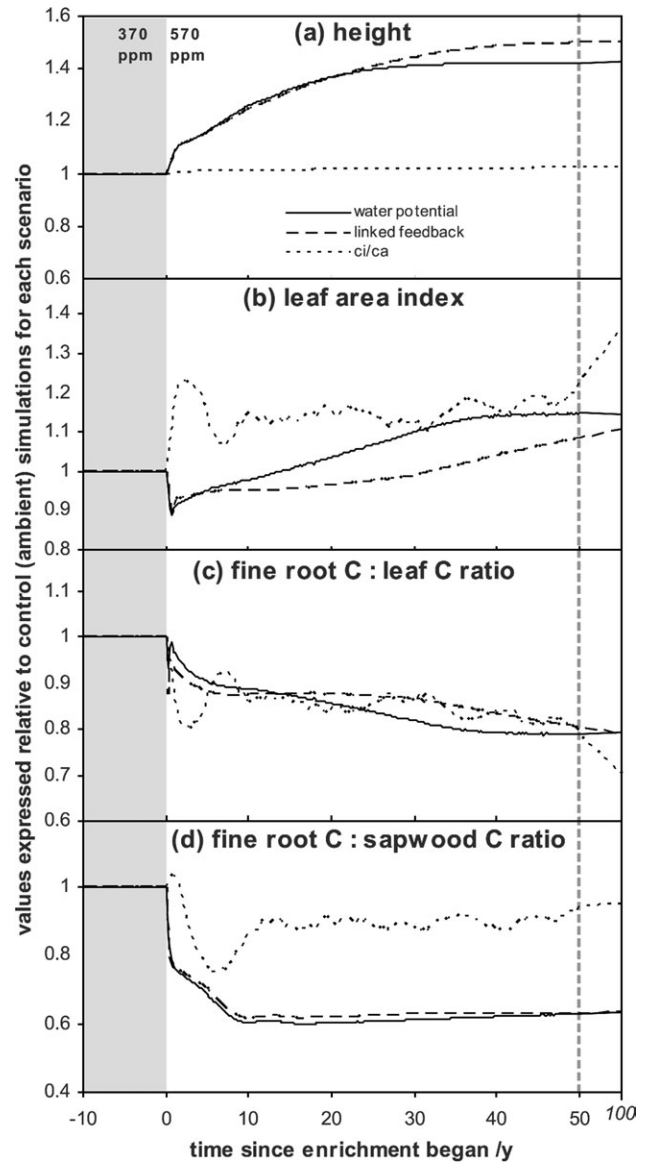


Fig. 1. Relative responses to a step change in ambient CO₂ from 370 ppm (shaded region) to 570 ppm (unshaded region) predicted by DESPOT for (a) tree height, (b) leaf area index, (c) ratio of fine root carbon to leaf carbon, and (d) ratio of fine root carbon to sapwood carbon. Three trajectories are shown in each panel, corresponding to three alternative constraints for stomatal acclimation: solid lines (ψ_1 -setpoint scenario: leaf water potential is constant); dashed lines [linked-feedback scenario: parameters of feedback model (Eqn 2) are constant]; and dotted lines (c_i/c_a -setpoint scenario: ratio of intercellular to ambient CO₂ mole fractions is constant). All responses are presented relative to control simulations in which ambient CO₂ remained at 370 ppm. To the right of the vertical dashed line at 50 years, the time axis is compressed, such that the next tick mark occurs at 100 years. Note that the vertical axis differs in each panel.

Figure 5 shows trajectories predicted for the marginal products for water, nitrogen, and light (μ_e , μ_n , and μ_l ; solid, dashed, and dotted lines in Fig. 5, respectively; Eqn 1), under each stomatal acclimation scenario. The general trend is identical in each scenario: μ_i increases strongly at first, then drops to near its initial value, while

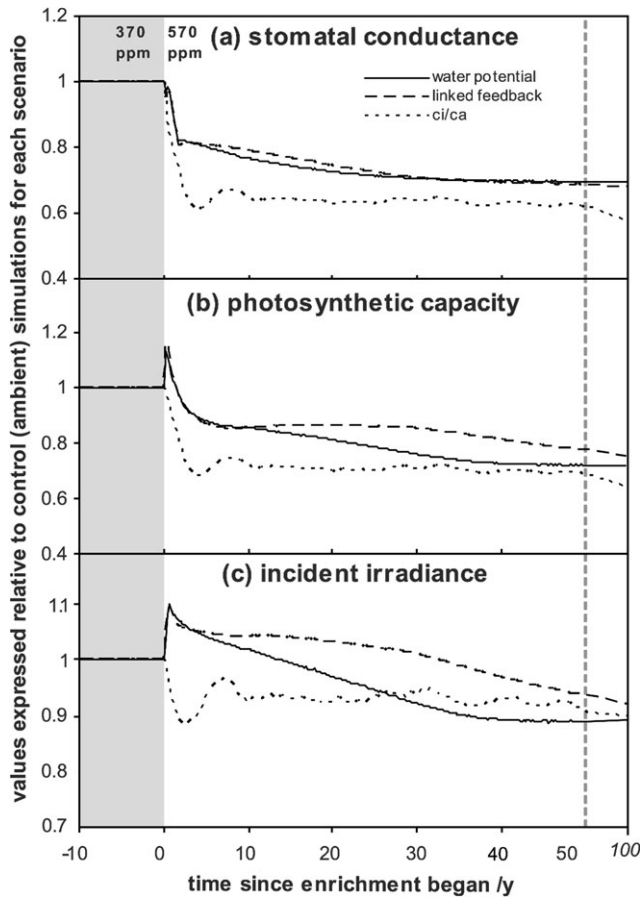


Fig. 2. Relative responses to CO₂ enrichment (step change from 370 ppm to 570 ppm at time zero) predicted by DESPOT for variables related to gas exchange: (a) stomatal conductance to water vapour (g_s), (b) photosynthetic capacity (carboxylation capacity, V_m), and (c) incident irradiance (photosynthetic photon flux density, I). The original values of g_s , V_m , and I are on a leaf area basis. Different line styles represent trajectories for three alternative stomatal acclimation constraints, as indicated by the inset legend in (a) and as described in the legend for Fig. 1. All responses are expressed relative to unenriched control simulations. The time axis from 50 to 100 years is compressed.

μ_n and μ_e increase less than μ_i but remain elevated. The eventual relative increase is greatest for μ_n , followed by μ_e and μ_i . In the c_i/c_a -setpoint scenario (Fig. 5b), μ_e and μ_n do not change after the initial response to enrichment, whereas μ_e and μ_n both fluctuate after enrichment in the ψ_1 and feedback scenarios (Fig. 5a and c, respectively), with μ_n decreasing and μ_e gradually increasing during height growth.

Discussion

No significant change in the ratio of c_i/c_a was predicted by DESPOT after several years of CO₂ enrichment, for any of the three alternative ‘setpoint’ assumptions used to constrain stomatal acclimation— c_i/c_a , ψ_1 , or the parameters of the linked hydraulic–biochemical feedback model for g_s (Eqn 2). This result is consistent with many data showing

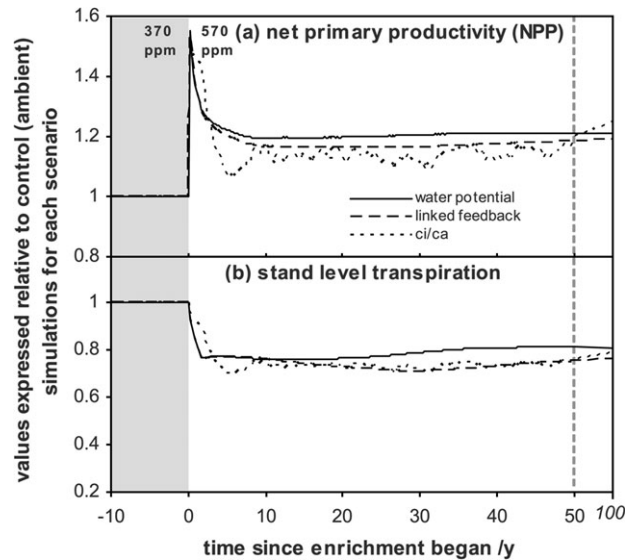


Fig. 3. Relative responses to CO₂ enrichment (step change from 370 ppm to 570 ppm at time zero) predicted by DESPOT for stand-level carbon and water fluxes: (a) net primary productivity (NPP) and (b) stand-level transpiration. Different line styles represent trajectories for three alternative stomatal acclimation constraints, as indicated by the inset legend in (a) and as described in the legend for Fig. 1. All responses are expressed relative to unenriched control simulations. The time axis from 50 to 100 years is compressed.

that the co-ordination of stomatal conductance and photosynthesis is usually not substantially altered by CO₂ enrichment (Ellsworth, 1999; Medlyn *et al.*, 2001; Schafer *et al.*, 2003; Herrick *et al.*, 2004; Ainsworth and Long, 2005). Several other predictions common to all three scenarios are also consistent with most observations from FACE experiments on trees (Ainsworth and Long, 2005): a decline in photosynthetic capacity (V_m), a somewhat larger decline in g_s , an eventual increase in LAI, and an enhancement of NPP that is greatest in the first year or two after enrichment, but which persists indefinitely at 14–21% above pre-enrichment values (Table 2).

Another prediction common to all three scenarios, that allocation to fine roots decreases relative to allocation to leaves or to sapwood, contradicts some results (Hyvonen *et al.*, 2007). One possible explanation for this is the lack of a mechanism for negative feedback between increased growth and nutrient availability in the model used here. However, reported enrichment responses for below-ground allocation are highly variable, with strong responses typically found in nutrient-limited conditions (Norby *et al.*, 2004) and small and ambiguous responses in the absence of container effects or prior nutrient limitations (Norby *et al.*, 1999; Tingey *et al.*, 2000; Hyvonen *et al.*, 2007). The fact that similar trends were predicted by each acclimation scenario for fine root allocation and NPP does suggest, at any rate, that variation in below-ground allocation responses is not related to variation in the character of stomatal acclimation, and that

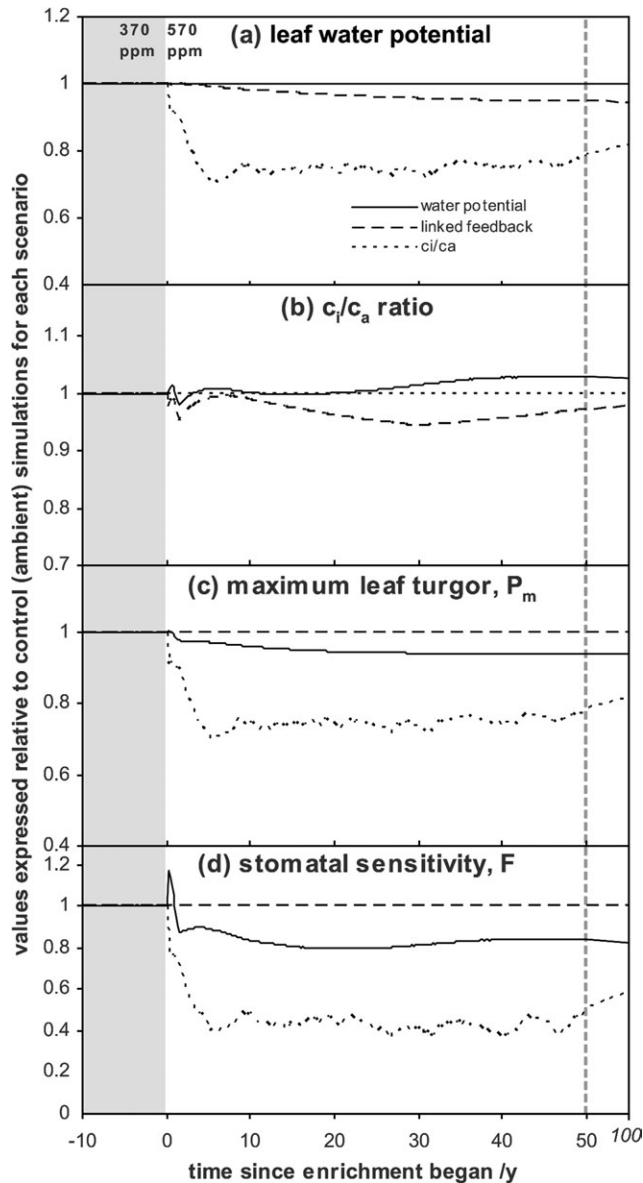


Fig. 4. Relative responses to CO₂ enrichment (step change from 370 ppm to 570 ppm at time zero) predicted by DESPOT for the parameters used as alternative setpoints for long-term stomatal acclimation: (a) leaf water potential (ψ_l , smaller values represent ψ_l closer to zero), (b) ratio of intercellular to ambient CO₂ mole fraction (c_i/c_a), and two parameters in the linked feedback model (Eqn 2) for stomatal control: (c) maximum leaf turgor (P_m), and (d) sensitivity (F) of stomatal conductance to leaf turgor and residual photosynthetic capacity. Different line styles represent simulations in which either ψ_l (solid lines), c_i/c_a (dotted lines), or both P_m and F (dashed lines) were held constant in order to constrain stomatal acclimation. All responses are expressed relative to unenriched control simulations. The time axis from 50 to 100 years is compressed.

none of the physiological constraints built into DESPOT should inherently prevent a sustained productivity enhancement of the same order as that observed in several forest FACE experiments ($23 \pm 2\%$) (Norby *et al.*, 2005).

The adaptive character of these responses can be interpreted in terms of changes in the sensitivities of carbon gain to water, nitrogen, and light (the marginal products

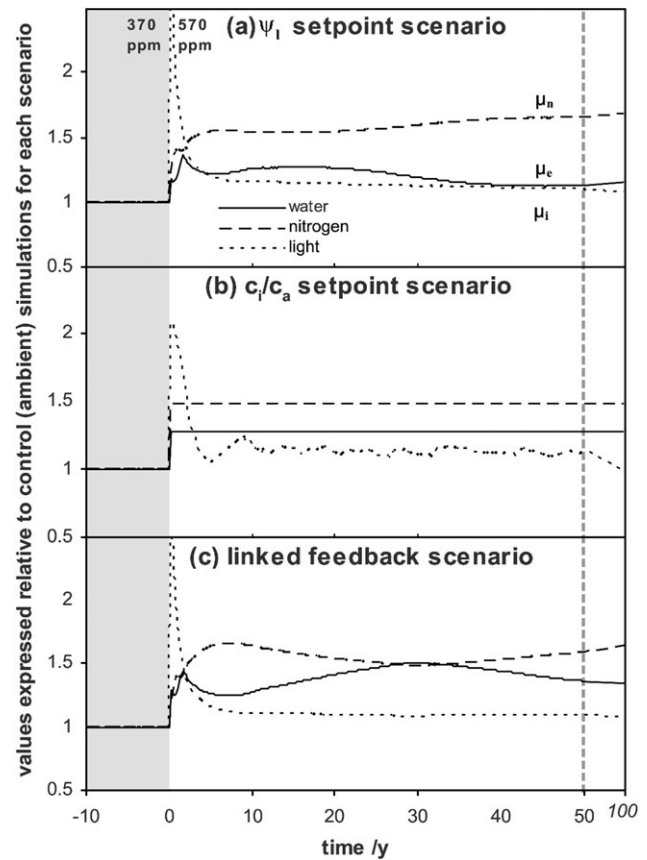


Fig. 5. Relative responses to CO₂ enrichment (step change from 370 ppm to 570 ppm at time zero) predicted by DESPOT for the marginal products of photosynthetic resources (Eqn 1) when different stomatal acclimation constraints were used in the model: (a) constant leaf water potential, ψ_l , (b) constant ratio of intercellular to ambient CO₂ mole fraction, c_i/c_a , or (c) constant parameters in the linked feedback model for stomatal control (Eqn 2). Different line styles represent marginal products for different resources: solid lines (marginal product for water, μ_w , $\partial A/\partial E$), dashed lines (marginal product for nitrogen, μ_n , $\partial A/\partial N$), dotted lines (marginal product for light, μ_l , $\partial A/\partial I$). All responses are expressed relative to unenriched control simulations. The time axis from 50 to 100 years is compressed.

μ_w , μ_n , and μ_l , respectively; Eqn 1 and Fig. 5), by reference to the equimarginal principle of production theory, which governs carbon allocation in the growth model used here. This principle states that the ratio of marginal product to marginal carbon cost should be the same for each photosynthetic resource. CO₂ enrichment initially causes a very large increase in μ_l relative to μ_w and μ_n (Fig. 5). Therefore, equimarginality requires either a shift in carbon allocation towards light capture, which would increase the marginal carbon cost of light, or an increase in leaf-level irradiance relative to V_m and g_s , which would reduce the marginal product for light relative to those for nitrogen and water. The increase in LAI (Fig. 1b) increases light capture, which works towards the first objective, and the reductions in V_m and g_s (Fig. 2a, b) both work towards the second objective. Enrichment also increases μ_n more than

Table 2. Comparison of enrichment responses observed for tree species in FACE experiments and those predicted by DESPOT using three different assumptions to constrain long-term stomatal acclimation

	Response to CO ₂ enrichment (%)				
	g_s	V_m	LAI	NPP	c_i/c_a
Observed^a					
All tree species	–15.6	–6.1	+21.0	+28.0 ^b	–1.9 ^c
Duke forest	–17.1	–5.9	0 ^d	+24 ^d	0 ^d
Predicted by DESPOT					
ψ_1 -setpoint scenario					
2 years	–17.3	–4.4	–7.7	+27.5	–1.2
5 years	–19.1	–12.0	–4.9	+22.3	+0.8
10 years	–22.6	–14.6	–2.2	+19.4	+0.1
50 years	–29.7	–28.3	+14.9	+21.0	+3.1
c_i/c_a -setpoint scenario					
2 years	–30.4	–23.0	+22.9	+35.8	0
5 years	–38.1	–31.5	+12.8	+6.7	0
10 years	–35.3	–28.4	+14.4	+15.0	0
50 years	–37.9	–31.3	+22.6	+19.8	0
Linked-feedback scenario					
2 years	–18.6	–5.4	–6.8	+26.1	–3.8
5 years	–18.8	–13.2	–5.6	+20.2	–0.9
10 years	–20.5	–14.8	–4.8	+16.6	–1.2
50 years	–30.6	–23.0	+8.2	+18.2	–2.9

^a Averages reported by Ainsworth and Long (2005) (AL), except ^d, which are from Schafer *et al.* (2003).

^b Reported by Ainsworth and Long (2005) as dry matter production.

^c A separate value was not reported by Ainsworth and Long (2005) for tree species; this is the value for all functional types. 2, 5, 10, and 50 years refer to values after enrichment began.

μ_e ; this dictates an increase in V_m relative to g_s , which explains why g_s declines more than V_m (Fig. 2a, b).

There was one fundamental difference in the enrichment responses predicted for the alternative scenarios for stomatal acclimation. The ψ_1 -setpoint and linked-feedback scenarios predicted a strong initial response of height growth followed by an increase in LAI, whereas the c_i/c_a -setpoint scenario predicted an immediate increase in LAI with no associated height growth response (Fig. 1a, b). Both of these responses—height growth and LAI enhancement—are driven by the initial increase in μ_i , which increases the profitability of light capture. Height growth eventually becomes less profitable due to increasing hydraulic burdens and respiratory costs, so allocation eventually shifts to leaf area production in the ψ_1 and feedback scenarios. The reason height growth did not respond in the c_i/c_a -setpoint scenario involves the effect on economic flexibility of treating c_i/c_a as a rigid setpoint. Height growth preferentially increases the marginal carbon cost of water (Buckley and Roberts, 2006b) so, in order for height growth to be economically efficient, the equimarginal principle requires substitution of light and/or nitrogen for water—or equivalently, of CO₂ demand for CO₂ supply. Treating c_i/c_a as a rigid setpoint precludes the required plasticity in CO₂ supply and demand. This makes height growth inherently less efficient in the c_i/c_a -setpoint

scenario, so DESPOT's optimization routine chooses to enhance leaf area rather than height growth in that scenario. The economic effect of this constraint is illustrated by the fact that μ_n and μ_e remain constant in the c_i/c_a scenario (Fig. 5b), whereas they change with respect to one another in relation to height growth dynamics in the ψ_1 and feedback scenarios (Fig. 5a, c).

This does not imply that the c_i/c_a -setpoint scenario is less representative of how real trees adapt to CO₂ enrichment, however. Reported LAI responses to enrichment in tree species are variable, with larger responses typically found for young trees in open stands (Kellomaki and Wang, 1997) or for mature stands with lower LAI (Norby *et al.*, 2005), and little or no response in mature forests with high LAI (Norby *et al.*, 2003; Schafer *et al.*, 2003). The present analysis suggests this variation may relate to plasticity in height growth, such that the initial responses of LAI and height to enrichment are anti-correlated among species. There are reasons to suspect that DESPOT's assumption of total plasticity in carbon allocation fractions overestimates the responsiveness of height growth to environmental change, particularly in mature trees. First, small reductions in either the flexibility or the precision of DESPOT's allocation algorithm cause NPP to decline with age, which the model does not otherwise predict (Buckley and Roberts, 2006a)—hinting that the model may indeed overestimate the plasticity of growth form in older trees. Secondly, McDowell *et al.* (2005) reported that carbon isotope discrimination was less sensitive to environmental change in tall Douglas-fir (*Pseudotsuga menziesii*) trees than in short trees, which they suggested may reduce the sensitivity of tall or otherwise hydraulically burdened trees to climate change.

Changes in stomatal function required to maintain ψ_1 or c_i/c_a -setpoints

The alternative setpoints can also be compared on the basis of their implications for stomatal physiology, because specific changes in the anatomical determinants of stomatal function are required to maintain fixed setpoints for either ψ_1 or c_i/c_a as tree structure and physiology adapt to CO₂ enrichment. A model based on the premise that stomatal control involves direct feedback responses to leaf turgor pressure and residual photosynthetic capacity (the 'linked-feedback' scenario, Eqn 2) (Jarvis and Davies, 1998; Buckley and Mott, 2002; Buckley, 2005) was used to infer how the parameters of those putative feedback responses—maximum turgor (P_m) and stomatal sensitivity (F) to the effectors of guard cell osmotic pressure—must vary during enrichment responses to preserve setpoints for ψ_1 or c_i/c_a . The parameter F captures changes in both stomatal density and the gain of guard cell signal transduction. The ψ_1 -setpoint scenario requires a 3–6% decline in P_m or a 9–16% decline in F ,

whereas the c_i/c_a -setpoint scenario requires a 25% decline in P_m or a 75% decline in F (Fig. 4b, c).

These predictions are difficult to validate or refute empirically, because little is known about the long-term acclimation in parameters that describe processes or properties directly involved in stomatal control. Stomatal density (embedded in F) is well known to decline in response to increasing c_a during growth; however, that response appears to saturate close to present-day ambient levels, and FACE experiments typically show little or no change in stomatal density (Medlyn *et al.*, 2001; Herrick *et al.*, 2004; Tricker *et al.*, 2005). Similarly, Herrick *et al.* (2004) found no effect of enrichment on the sensitivity of g_s to soil moisture or evaporative gradient in sweetgum (*Liquidambar styraciflua*) trees in the Duke FACE experiment, and Leakey *et al.* (2006) found that short-term stomatal responses in enriched soybean (*Glycine max*) plants were accurately described using the Ball–Berry model with pre-enrichment parameter values. These results suggest, but by no means prove, that the reduced parameters of stomatal function are not strongly sensitive to CO₂ enrichment above present-day levels.

This supports the linked-feedback scenario, which assumes that P_m and F do not respond to enrichment. In contrast, the ψ_1 - and c_i/c_a -setpoint scenarios both require either P_m or F to change after enrichment. The required change is smaller for P_m than for F in both cases, suggesting that either setpoint scenario is more likely to involve osmotic down-regulation (i.e. reductions in maximum leaf turgor, P_m) than reductions in stomatal density or guard cell metabolic sensitivity. Additionally, much smaller changes in P_m and F are required to preserve a constant setpoint for ψ_1 than for c_i/c_a . The matter could be clarified by characterizing in greater detail how enrichment affects stomatal properties in trees, ideally in the language of a process-based model. It is interesting to note that the linked-feedback scenario (fixed P_m and F) predicts trajectories for both ψ_1 and c_i/c_a that remain within $\pm 5\%$ of their pre-enrichment values (Fig. 5a, b). This prediction is intriguing because it shows that conservative behaviour in the apparent hydraulic and biochemical setpoints of stomatal control can emerge passively from local feedback regulation—without the need for any systemic co-ordination or acclimation of stomatal physiology, and even after a 200 ppm increase in c_a .

Recommendations for model-based prediction and analysis

The analysis presented above leads to two conclusions relevant to the choice of stomatal constraints in models used to interpret or simulate tree responses to CO₂ enrichment. First, the adaptive landscape on which growth and gas exchange are regulated is strongly affected by *a priori* constraints on the phenomenological *outcomes* of struc-

tural and physiological adaptation. A constant ratio of c_i/c_a , for example, precludes resource substitution between nitrogen and water, which in turn leads to very different predictions for both the timing and magnitude of acclimatory adjustments in LAI and tree height to enrichment. Secondly, if constraints are based on the regulatory processes that are hypothesized to give rise to homeostatic setpoints, rather than on the assumption that those setpoints will be preserved, the long-term behaviour that emerges for those setpoints turns out to be quite conservative anyway. The recommendation arising from these conclusions depends on the reason for which one is simulating tree responses to CO₂ in the first place. Any process-based model, even the simple conceptual ‘linked-feedback’ model used here, increases computational time and complexity, and the results of this study suggest that the phenomenology that emerges from such models is very similar to that embedded in setpoint assumptions anyway. Therefore, when the purpose of modelling is simply to project gas exchange dynamics under high CO₂, this study offers no reason to abandon the simplicity and computational efficiency offered by setpoint assumptions. If, on the other hand, the purpose of modelling is to understand the interplay between physiological and structural responses to CO₂ enrichment—particularly from an adaptive or economic perspective—a more wary approach to ‘setpoints’ is warranted. Understanding of these issues could be improved by experiments designed to characterize stomatal acclimation in terms of reduced properties related to the processes involved in stomatal control, and by experiments designed to quantify the plasticity of carbon allocation, particularly height growth, with respect to the drivers of photosynthetic resource balance.

Conclusions

Adaptive tree responses to a step increase in ambient CO₂ from 370 ppm to 570 ppm were simulated with an optimality-based growth model, using three alternative ‘setpoints’ for stomatal acclimation: leaf water potential (ψ_1), the ratio of intercellular to ambient CO₂ mole fraction (c_i/c_a), or the parameters of a simple feedback model for stomatal control (Eqn 2). None of the scenarios predicted large changes in the co-ordination of stomatal conductance with photosynthesis (as c_i/c_a) in the first decade after enrichment. All scenarios predicted declines in g_s and V_m , and increases in NPP and LAI as reported in FACE experiments. The LAI response was initially offset by diversion of carbon for height growth in the ψ_1 and feedback scenarios, but not in the c_i/c_a scenario. Both responses (LAI and height growth) served to re-establish equimarginality by shifting photosynthetic resource balance towards light, after the CO₂ enrichment-induced jump in the marginal product for light. Height growth also requires

substitution of N for water, which is impossible if c_i/c_a is fixed, explaining the lack of height response in the c_i/c_a scenario. Conservative behaviour for c_i/c_a was predicted in the ψ_1 -setpoint and feedback scenarios, and all scenarios predicted similar long-term behaviour for stand-level carbon and water fluxes and above- versus below-ground partitioning. These results suggest that c_i/c_a or ψ_1 could be used as setpoints for constraining flux projections. However, they also highlight the importance of *a priori* constraints on allocation and co-ordination in determining patterns of structural and physiological adjustment. This suggests that the adaptive or physiological basis of those patterns cannot be fully understood without a better understanding of the process basis of stomatal acclimation itself.

Acknowledgements

I thank James Morison, Gabriel Cornic, and the organizers of the 14th International Congress on Photosynthesis for the invitation to submit this article. This work was funded by the Highfire Project of Australia's Bushfire Cooperative Research Centre.

Appendix

Gas exchange model

The calculations described in this paper, including those embedded in the DESPOT model, were based on the photosynthesis model of Farquhar *et al.* (1980), combined with simplified Fick's Law-based diffusion models for CO₂ and water vapour flux between leaves and the atmosphere. Net CO₂ assimilation rate is defined by the intersection of mesophyll demand (A_d) and stomatal diffusion (supply, A_s):

$$A = A_d \cap A_s \quad (\text{A1})$$

$$A_s = g(c_a - c_i) \quad (\text{A2})$$

$$A_d = \min\{A_v, A_j, \theta_A\} \quad (\text{A3})$$

where g is total conductance to CO₂, $\min\{y,z,\theta\}$ is defined as the lesser solution X of $\theta X^2 - (y+z)X + yz = 0$, and A_v and A_j are RuBP carboxylation- and regeneration-limited assimilation rates, respectively:

$$A_v = \frac{V_m(c_i - \Gamma_*)}{c_i + K'} - R_d \quad (\text{A4})$$

$$A_j = \frac{1}{4} - \frac{J(c_i - \Gamma_*)}{c_i + 2\Gamma_*} - R_d \quad (\text{A5})$$

where V_m is maximum carboxylation velocity, R_d is the rate of mitochondrial respiration that continues in the dark

(assumed equal to $0.01 \times V_m$), K' is the effective Michaelis constant for carboxylation by Rubisco, Γ_* is the photo-respiratory compensation point, and J is the potential electron transport rate, given by $J = \min\{J_m, \phi I, \theta_j\}$; J_m is the maximum potential electron transport rate, I is incident PPFD, ϕ is effective maximum quantum yield of electron transport from incident PPFD, and θ_j is a curvature parameter (0.9). V_m and J_m are considered proportional to leaf N content, N ($V_m = \chi_v N$ and $J_m = \chi_j N$), which in turn is the ratio of canopy N content to leaf area ($N = N_t/L$). In DESPOT, $\chi_j = 1.9 \mu\text{mol e}^- \text{mmol}^{-1} \text{N}$ and $\chi_v = \chi_j / (2.1 \text{ e}^-/\text{CO}_2)$. Incident PPFD, I , is annual canopy PPFD capture divided by leaf area and by a time integration factor Y [Y represents, in essence, the number of seconds of positive photosynthesis each year; see Buckley and Roberts (2006a) for details] ($I = I_t/L$). g is annual canopy transpiration (E_t) divided by leaf area, Y and $1.6 \times D$ [$g = E_t / (1.6 \times DLY)$], where D is leaf–air H₂O mole fraction difference and 1.6 converts from H₂O to CO₂ diffusivity. Note that this assumes negligible boundary layer resistance. Calculating E , N , and I from E_t , N_t , and I_t in this way is equivalent to a 'big-leaf' assumption, i.e. the gas exchange model is assumed to be scale-invariant (Farquhar, 1989; Field, 1991).

Note that for $\theta_A < 1$, the intersection of Eqns A2 and A3 creates a *quartic* expression for c_i , which can be solved directly as described in any mathematics text. It would be simpler to calculate the intersections of A_s with A_j and A_v separately and then take the minimum; however, this is strictly incorrect if $\theta_A < 1$, and it creates discontinuous marginal products if θ_A is assumed equal to 1. In reality, there will always be some co-limitation, however small, between carboxylation and regeneration, and although accommodating $\theta_A < 1$ is more difficult computationally, meaningful analysis of photosynthetic resource economics is otherwise impossible. In the present study θ_A was assumed to be equal to 0.9.

Marginal products

The marginal products from water, nitrogen, and light (transpiration, photosynthetic leaf N content, and incident PPFD, to be precise) can be calculated from the gas exchange model described above. Only the final expressions are given here; see Buckley *et al.* (2002) for complete derivations. The marginal product from water use is

$$\mu_e \equiv \frac{\partial A}{\partial E} = \frac{k}{g + k} \left(\frac{A}{E} \right) \quad (\text{A6})$$

where k is the slope of the photosynthetic demand curve, calculated as described below (Eqns A12–A14). Note that, like the gas exchange model itself, Eqn A6 assumes that the canopy is well coupled to the atmosphere. This avoids complications arising from the different ratios of

diffusivities for H₂O and CO₂ for diffusion and bulk flow, and from effects of changes in leaf temperature on VPD and photosynthetic parameters. Expressions that accommodate such effects are given by Buckley *et al.* (2002). The marginal product from photosynthetic N use is a function of two values, $\mu_{n,v}$ and $\mu_{n,j}$, representing carboxylation- and regeneration-limited conditions, respectively:

$$\mu_n = \frac{\mu_{n,j}(A - A_v) + \mu_{n,v}(A - A_j)}{2\theta_A A - A_v - A_j} \quad (\text{A7})$$

$$\mu_{n,j} \equiv \frac{\partial A_j}{\partial N} = \frac{g}{g+k} \left[\left(\frac{A_j + R_d}{J} \right) \left(\frac{J - \phi I}{2\theta_j J - J_m - \phi I} \right) \chi_j - 0.01 \chi_v \right] \quad (\text{A8})$$

$$\mu_{n,v} \equiv \frac{\partial A_v}{\partial N} = \frac{g}{g+k} \left(\frac{A_v}{N} \right) \quad (\text{A9})$$

Equation A7 is found by implicitly differentiating the *minh* function. The marginal product from PPF requires a similar calculation, except that the value corresponding to carboxylation-limited conditions is simply zero ($\mu_{i,v}=0$):

$$\mu_i = \frac{\mu_{i,j}(A - A_v)}{2\theta_A A - A_v - A_j} \quad (\text{A10})$$

$$\mu_{i,j} \equiv \frac{\partial A_j}{\partial I} = \frac{g}{g+k} \left(\frac{A_j + R_d}{J} \right) \cdot \left(\frac{J - J_m}{2\theta_j J - J_m - \phi I} \right) \phi \quad (\text{A11})$$

Finally, the slope of the demand curve, k , is calculated in similar fashion, from values (k_v and k_j) representing the different limitations:

$$k \equiv \left(\frac{\partial A}{\partial c_i} \right)_{N,I} = \frac{\partial A_d}{\partial c_i} = \frac{k_j(A - A_v) + k_v(A - A_j)}{2\theta_A A - A_v - A_j} \quad (\text{A12})$$

$$k_v = \frac{V_m(K' + \Gamma^*)}{(c_i + K')^2} \quad (\text{A13})$$

$$k_j = \frac{3}{4} \frac{J\Gamma^*}{(c_i + 2\Gamma^*)^2} \quad (\text{A14})$$

References

- Ainsworth EA, Long S. 2005. What have we learned from 15 years of free-air CO₂ enrichment (FACE)? A meta-analytic review of the responses of photosynthesis, canopy properties and plant production to rising CO₂. *New Phytologist* **165**, 351–372.
- Barnard HR, Ryan MG. 2003. A test of the hydraulic limitation hypothesis in fast-growing *Eucalyptus saligna*. *Plant, Cell and Environment* **26**, 1235–1245.
- Battaglia M, Sands P, White D, Mummery D. 2004. CABALA: a linked carbon, water and nitrogen model of forest growth for silvicultural decision support. *Forest Ecology and Management* **193**, 251–282.
- Buckley TN. 2005. The control of stomata by water balance (Tansley Review). *New Phytologist* **168**, 275–292.
- Buckley TN, Miller JM, Farquhar GD. 2002. The mathematics of linked optimisation for nitrogen and water use in a canopy. *Silva Fennica* **36**, 639–669.
- Buckley TN, Mott KA. 2002. Stomatal water relations and the control of hydraulic supply and demand. *Progress in Botany* **63**, 309–325.
- Buckley TN, Mott KA, Farquhar GD. 2003. A hydromechanical and biochemical model of stomatal conductance. *Plant, Cell and Environment* **26**, 1767–1785.
- Buckley TN, Roberts DW. 2006a. DESPOT, a process-based tree growth model that allocates carbon to maximize carbon gain. *Tree Physiology* **26**, 129–144.
- Buckley TN, Roberts DW. 2006b. How should leaf area, sapwood area and stomatal conductance vary with tree height to maximise growth? *Tree Physiology* **26**, 145–157.
- Davidson RL. 1969. Effect of root/leaf temperature differentials on root/shoot ratios in some pasture grasses and clover. *Annals of Botany* **33**, 561–569.
- Deleuze C, Houllier F. 1995. Prediction of stem profile of *Picea abies* using a process-based tree growth model. *Tree Physiology* **15**, 113–120.
- Ehleringer JR, Cerling TE. 1995. Atmospheric CO₂ and the ratio of intercellular to ambient CO₂ concentrations in plants. *Tree Physiology* **15**, 105–111.
- Ellsworth DS. 1999. CO₂ enrichment in a maturing pine forest: are CO₂ exchange and water status in the canopy affected? *Plant, Cell and Environment* **22**, 461–472.
- Farquhar GD. 1989. Models of integrated photosynthesis of cells and leaves. *Philosophical Transactions of the Royal Society B: Biological Sciences* **323**, 357–367.
- Farquhar GD, Ehleringer JR, Hubick KT. 1989. Carbon isotope discrimination and photosynthesis. *Annual Review of Plant Physiology and Plant Molecular Biology* **40**, 503–537.
- Farquhar GD, Sharkey TD. 1982. Stomatal conductance and photosynthesis. *Annual Review of Plant Physiology* **33**, 317–345.
- Farquhar GD, von Caemmerer S, Berry JA. 1980. A biochemical model of photosynthetic CO₂ assimilation in leaves of C₃ species. *Planta* **149**, 78–90.
- Field CB. 1991. Ecological scaling of carbon gain to stress and resource availability. In: Mooney HA, Winner WE, Pell EJ, eds. *Response of plants to multiple stresses*. San Diego: Academic Press, 35–65.
- Grote R. 1998. Integrating dynamic morphological properties into forest growth modeling. II. Allocation and mortality. *Forest Ecology and Management* **111**, 193–210.
- Herrick JD, Maherali H, Thomas RB. 2004. Reduced stomatal conductance in sweetgum (*Liquidambar styraciflua*) sustained over long-term CO₂ enrichment. *New Phytologist* **162**, 387–396.
- Hilbert DW, Reynolds JF. 1991. A model allocating growth among leaf proteins, shoot structure, and root biomass to produce balanced activity. *Annals of Botany* **68**, 417–425.
- Hyvonen R, Agren GI, Linder S, *et al.* 2007. The likely impact of elevated [CO₂], nitrogen deposition, increased temperature and management on carbon sequestration in temperate and boreal forest ecosystems: a literature review. *New Phytologist* **173**, 463–480.

- Jarvis AJ, Davies WJ. 1998. The coupled response of stomatal conductance to photosynthesis and transpiration. *Journal of Experimental Botany* **49**, 399–406.
- Jones HG. 1990. Physiological aspects of the control of water status in horticultural crops. *Horticultural Science* **25**, 19–26.
- Kellomaki S, Wang KY. 1997. Effects of long-term CO₂ and temperature elevation on crown nitrogen distribution and daily photosynthetic performance of Scots pine. *Forest Ecology and Management* **99**, 309–326.
- Korner C. 2006. Plant CO₂ responses: an issue of definition, time and resource supply. *New Phytologist* **172**, 393–411.
- Korner C, Asshoff R, Bignucolo O, Hattenschwiler S, Keel SG, Pelaez-Riedl S, Pepin S, Siegwolf RTW, Zott G. 2005. Carbon flux and growth in mature deciduous forest trees exposed to elevated CO₂. *Science* **309**, 1360–1362.
- Leakey ADB, Bernacchi CJ, Ort DR, Long SP. 2006. Long-term growth of soybean at elevated [CO₂] does not cause acclimation of stomatal conductance under fully open-air conditions. *Plant, Cell and Environment* **29**, 1794–1800.
- Lo E, Zhang MW, Lechowicz M, Messier C, Nikinmaa E, Perttunen J, Sievanen RP. 2001. Adaptation of the LIGNUM model for simulations of growth and light response in Jack pine. *Forest Ecology and Management* **150**, 279–291.
- Luan J, Muetzelfeldt RI, Grace J. 1996. Hierarchical approach to forest ecosystem simulation. *Ecological Modelling* **86**, 37–50.
- Mäkelä A. 1986. Implications of the pipe model theory on dry matter partitioning and height growth in trees. *Journal of Theoretical Biology* **123**, 103–120.
- Mäkelä AA. 1997. A carbon balance model of growth and self-pruning in trees based on structural relationships. *Forest Science* **43**, 7–24.
- Mäkelä A. 1999. Acclimation in dynamic models based on structural relationships. *Functional Ecology* **13**, 145–156.
- McDowell NG, Licata J, Bond BJ. 2005. Environmental sensitivity of gas exchange in different-sized trees. *Oecologia* **145**, 9–20.
- Medlyn BE, Barton CVM, Broadmeadow M, et al. 2001. Stomatal conductance of forest species after long-term exposure to elevated CO₂ concentration: a synthesis. *New Phytologist* **149**, 247–264.
- Miller JM. 2002. *Carbon isotope discrimination by Eucalyptus species*. The Australian National University, Canberra, 258.
- Miller JM, Williams RJ, Farquhar GD. 2001. Carbon isotope discrimination by a sequence of *Eucalyptus* species along a sub-continental rainfall gradient in Australia. *Functional Ecology* **15**, 222–232.
- Norby RJ, DeLucia EH, Gielen B, et al. 2005. Forest response to elevated CO₂ is conserved across a broad range of productivity. *Proceedings of the National Academy of Sciences, USA* **102**, 18052–18056.
- Norby RJ, Ledford J, Reilly CD, Miller NE, O'Neill EG. 2004. Fine-root production dominates response of a deciduous forest to atmospheric CO₂ enrichment. *Proceedings of the National Academy of Sciences, USA* **101**, 9689–9693.
- Norby RJ, Sholtis JD, Gunderson CA, Jawdy SS. 2003. Leaf dynamics of a deciduous forest canopy: no response to elevated CO₂. *Oecologia* **136**, 574–584.
- Norby RJ, Wullschlegel SD, Gunderson CA, Johnson DW, Ceulemans R. 1999. Tree responses to rising CO₂ in field experiments: implications for the future forest. *Plant, Cell and Environment* **22**, 683–714.
- Phillips N, Bond BJ, McDowell NG, Ryan MG, Schauer A. 2003. Leaf area compounds height-related hydraulic costs of water transport in Oregon White Oak trees. *Functional Ecology* **17**, 832–840.
- Ryan MG, Phillips N, Bond BJ. 2006. The hydraulic limitation hypothesis revisited. *Plant, Cell and Environment* **29**, 367–381.
- Saliendra NZ, Sperry JS, Comstock JP. 1995. Influence of leaf water status on stomatal response to humidity, hydraulic conductance, and soil drought in *Betula occidentalis*. *Planta* **196**, 357–366.
- Schafer KVR, Oren R, Ellsworth DS, Lai C-T, Herrick JD, Finzi AC, Richter DD, Katul GG. 2003. Exposure to an enriched CO₂ atmosphere alters carbon assimilation and allocation in a pine forest ecosystem. *Global Change Biology* **9**, 1378–1400.
- Shinozaki K, Yoda K, Hozumi K, Kira T. 1964a. A quantitative analysis of plant form: the pipe model theory. I. Basic analysis. *Japanese Journal of Ecology* **14**, 97–105.
- Shinozaki K, Yoda K, Hozumi K, Kira T. 1964b. A quantitative analysis of plant form: the pipe model theory. II. Further evidence of the theory and its application in forest ecology. *Japanese Journal of Ecology* **14**, 133–139.
- Steffen W, Canadell P. 2005. *Carbon dioxide fertilisation and climate change policy*. Canberra: Australian Greenhouse Office.
- Tardieu F. 1993. Will increases in our understanding of soil–root relations and root signalling substantially alter water flux models? *Philosophical Transactions of the Royal Society B: Biological Sciences* **341**, 57–66.
- Thornley JHM. 1972a. A balanced quantitative model for root: shoot ratios in vegetative plants. *Annals of Botany* **36**, 431–441.
- Thornley JHM. 1972b. A model to describe the partitioning of photosynthate during vegetative growth. *Annals of Botany* **33**, 419–430.
- Tingey DT, Phillips DL, Johnson MG. 2000. Elevated CO₂ and conifer roots: effects on growth, life span and turnover. *New Phytologist* **147**, 87–103.
- Tricker PJ, Trewin H, Kull O, Clarkson GJJ, Eensalu E, Tallis MJ, Colella A, Doncaster CP, Sabatti M, Taylor G. 2005. Stomatal conductance and not stomatal density determines the long-term reduction in leaf transpiration of poplar in elevated CO₂. *Oecologia* **143**, 652–660.
- Valentine H. 1985. Tree-growth models: derivations employing the pipe-model theory. *Journal of Theoretical Biology* **117**, 579–585.
- Valentine H. 1999. Estimation of the net primary productivity of even-aged stands with a carbon-allocation model. *Ecological Modelling* **122**, 139–149.
- Wong SC, Cowan IR, Farquhar GD. 1979. Stomatal conductance correlates with photosynthetic capacity. *Nature* **282**, 424–426.
- Wong SC, Cowan IR, Farquhar GD. 1985b. Leaf conductance in relation to rate of CO₂ assimilation. I. Influence of nitrogen nutrition, phosphorus nutrition, photon flux density, and ambient partial pressure of CO₂ during ontogeny. *Plant Physiology* **78**, 821–825.
- Wong SC, Cowan IR, Farquhar GD. 1985b. Leaf conductance in relation to rate of CO₂ assimilation. III. Influences of water stress and photoinhibition. *Plant Physiology* **78**, 830–834.